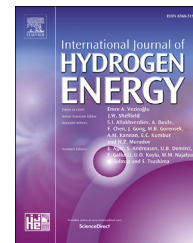Available online at www.sciencedirect.com

ScienceDirect

journal homepage: www.elsevier.com/locate/he

Mechanical strength improvement of aluminum foam-reinforced matrix for molten carbonate fuel cells

CrossMark

Mihui Lee [a,b], *Chang-Whan Lee* [c], *Hyung-Chul Ham* [a], *Jonghee Han* [a], *Sung Pil Yoon* [a,*], *Ki Bong Lee* [b]

[a] *Fuel Cell Research Center, Korea Institute of Science and Technology (KIST), Harang-ro 14-gil 5, Seongbuk-gu, Seoul 02792, Republic of Korea*
[b] *Department of Chemical and Biological Engineering, Korea University, 145 Anam-ro, Seongbuk-gu, Seoul 02841, Republic of Korea*
[c] *Department of Mechanical System Design Engineering, Seoul National University of Science and Technology, 232 Gongneung-ro, Nowon-gu, Seoul 01811, Republic of Korea*

ARTICLE INFO

ABSTRACT

During the cell operation of molten carbonate fuel cells (MCFCs), matrix cracks caused by poor mechanical strength accelerate cell performance degradation. Therefore, for a stable long-term cell operation, the improvement of mechanical properties of matrix is highly required. In this study, aluminum foam was used to enhance the mechanical strength of the matrix as a 3D (three dimensional) support structure. Unlikely conventional matrix (pure α-LiAlO$_2$ matrix) which has paste-like structure at the MCFC operating temperature, Al foam-reinforced α-LiAlO$_2$ matrix has significantly strong mechanical strength because the 3D network structure of Al foam can form the harden alumina skin layer during a cell operation. As a result, the mechanical strength of the Al foam-reinforced α-LiAlO$_2$ matrix was enhanced by 9 times higher than the pure α-LiAlO$_2$ matrix in a 3-point bending test. In addition, thermal cycle test showed notable cell stability due to strong mechanical strength of Al foam-reinforced α-LiAlO$_2$ matrix. The Al foam-reinforced α-LiAlO$_2$ matrix shows appropriate microstructure to preserve the liquid electrolyte when performing the mercury porosimeter analysis and differential pressure test between anode and cathode. Moreover, evaluation of stability and durability for a long-term cell operation were demonstrated by single cell test for 1,000 h.

Introduction

Technology and materials of MCFC have developed from 1980s to early 1990s by the worldwide attention and funding [1]. Due to the high operating temperature of MCFC, electrochemical reaction at the electrodes is relatively fast, therefore low priced materials, such as nickel and nickel oxide, can be used as electrodes. Moreover, since the internal reforming is applicable, including the hydrogen, carbon monoxide, and methane, the other gas fuels can be introduced as fuels. In addition, utilization of the waste heat from the

high operating temperature is practicable to increase power generation efficiency. Nevertheless, competition with the other renewable energy systems is uncertain, because it is still in initial stage of commercial validity [2]. Moreover, limited cell & stack lifetime, low power density and costs problems are required to be solved as well. Especially, 40,000 h of operation time is required for commercialization of MCFC [3]. For a stable long-term operation of cell, gas crossover by matrix cracking, electrolyte loss, structural deformation of anode by creep and sintering, and cathode dissolution, and corrosion caused by high operation temperature are necessary to be studied to determine validity of stability and durability.

The matrix can play a role as the porous ceramic support for holding the liquid molten carbonates. The matrix is a pathway of CO_3^{2-} ion from cathode to anode insulating the electrodes electrically. In addition, the matrix filled up with electrolyte prevents the mixing of reactants inside of the cell, such as fuel and air from flowing into each electrode in the cell, and it also behaves as a wet seal to prevent gas escaping to the outside of the cell. For the most requirements of matrix for MCFCs, they are strongly related to the physical properties and not to the electrochemical properties of matrix. Therefore, it is required for matrix to have proper mechanical strength in order to endure the cracking or structure alteration resulted by mechanical stress or thermal stress during the cell operation.

Some researchers have suggested several approaches to enhance the mechanical strength of matrix. J.-J. Lee et al. [4] have evaluated the improvement by melting and phase transition of the aluminum from addition of different sized aluminum particles. H.C. Hahm et al. [5] have investigated the developed mechanical properties by liquid-phase sintering of B_2O_3. I. Lee et al. [6] have studied the enhancement with aluminum acetylacetonate by neck formation among $LiAlO_2$ particles. In addition, H.-S. Kim et al. [7] increased the strength with nano sized aluminum particles by forming bridge between $LiAlO_2$ particles. J.-E. Kim et al. [8] have investigated mechanical strength enhancement by metal wire mesh. Furthermore, J.-E. Kim et al., and Patil KY et al. [9,10] have demonstrated the adding Li ion source to prevent the Li_2CO_3 depletion from lithiated aluminum reaction due to aluminum adding for the matrix.

In this study, aluminum foam was used as a 3D network support to reinforce mechanical strength of the matrix. Since the surface of Al foam can be oxidized to alumina skin layer during a cell operation, it can be suggested that the Al foam-matrix shows good mechanical strength to reduce the cracks caused by mechanical stress and thermal stress for a long-term cell operation. Schematic illustration of Al foam-reinforced α-$LiAlO_2$ matrix is demonstrated in Fig. 1.

Experimental

Fabrication of matrix

The pure α-$LiAlO_2$ matrix, as a standard matrix, was fabricated by tape casting method [11]. For the slurry procedure of pure α-$LiAlO_2$ matrix, alpha lithium aluminate (Alpha-10, Chemetall
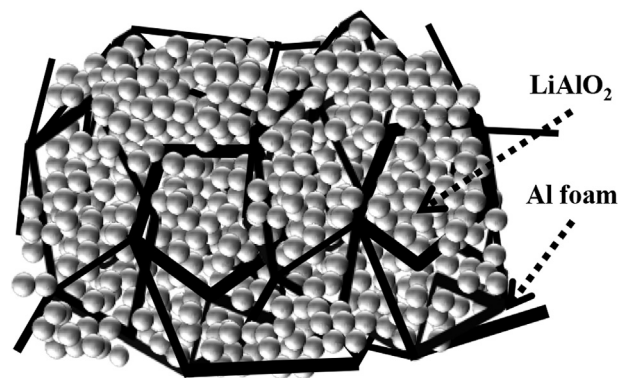

Fig. 1 – Schematic illustration of Al foam-reinforced α-$LiAlO_2$ matrix.

Foote Corp., Germany), binder (Butavar B76, Eastman Chemical Company, USA), plasticizer (dibutyl phthalate 99.0%+, Junsei, Japan), defoamer (SN D-348, San Nopco Korea LTD., Republic of Korea), dispersant (BYK110, BYK Additives and Instruments), and solvent mixture of ethyl alcohol (99.9%, anhydrous, Samchun, Republic of Korea) and toluene (99.5%, Samchun, Republic of Korea) in weight ratio of 7:3 are used and then the slurry was ball-milled for 48 h twice.

In order to fabricate Al foam-reinforced α-$LiAlO_2$ matrix, Al foam (Al-6101-T6, Duocel, ERG Oakland, USA) was used. The aluminum foam is a cellular structure of aluminum with 91% of porosity, and 40 PPI (pores per inch) of pores size consisting of 98.5% of aluminum. The surface of aluminum foam was pre-oxidized at 800 °C for 3 h to prevent the deformation in the heat-up procedure for cell operation due to Al melting and to improve the wettability to the electrolyte for good impregnation. After the pre-oxidation procedure, the Al foam was oxidized with alumina skin layer in the thickness of 1 μm. The surface morphologies of Al foam before and after the pre-oxidation procedure are compared in Fig. 2. And then, the pores of oxidized aluminum foam were packed with the pure α-$LiAlO_2$ slurry by vacuum suction of 0.6 bar for 20 min. After drying the pure α-$LiAlO_2$ slurry supported by aluminum foam, the Al foam-reinforced α-$LiAlO_2$ matrix was obtained. The overall fabrication process of Al foam-reinforced α-$LiAlO_2$ matrix is shown in Fig. 3, and the slurry composition of pure α-$LiAlO_2$ matrix to pack the Al foam is summarized in Table 1.

Characterization

To examine the physical characteristics of matrix, the matrix samples were burned out at 620 °C for 3 h to remove the organics in the matrix. First, the matrix morphology was observed by scanning electron microscopy (FE-SEM; Inspect F, FEI, USA). Since pore properties of matrix are important to control electrolyte retention capacity, porosity and pore size distribution were analyzed by mercury porosimeter (AutoPore IV 9500 series, Micromeritics Instrument Co., USA). By calculation with the mercury porosimeter result, all pores of matrix were filled up with the electrolyte for 100.

In addition, differential pressure test between anode and cathode outlets was carried out to investigate the electrolyte retention capacity of the matrix during the cell operation at
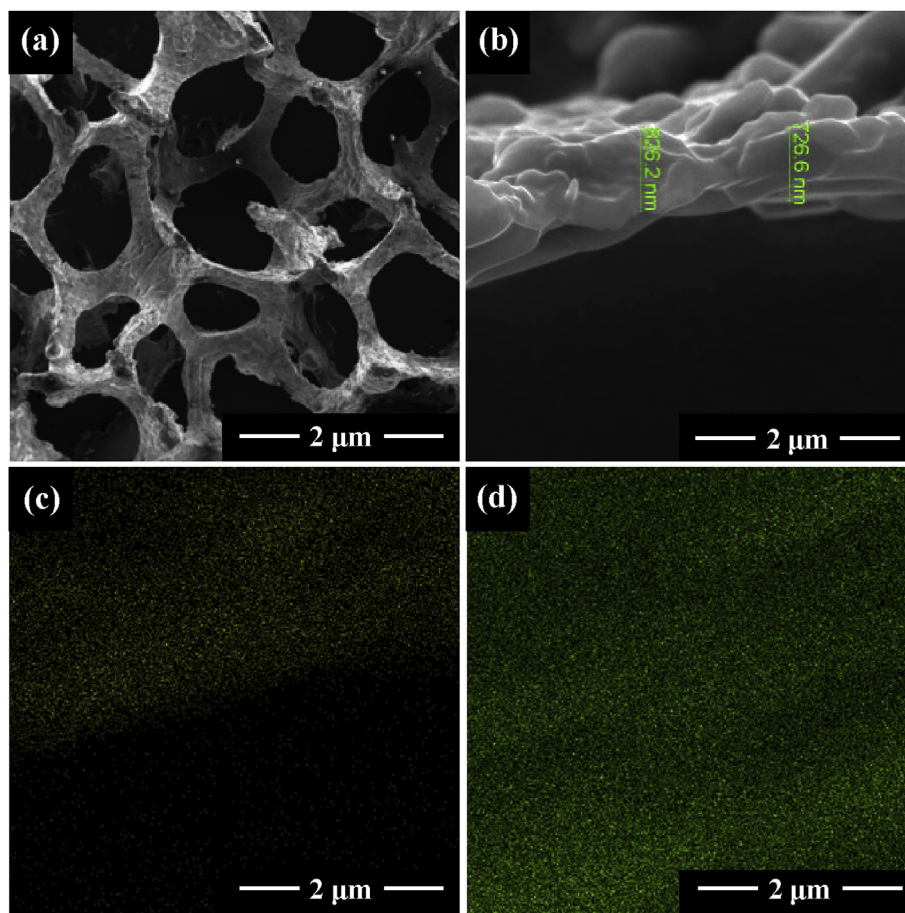
Fig. 2 − SEM images of (a) Al foam, and (b) Al foam after oxidation, EDS images of (c) element O mapping of the (b), and (d) element Al mapping of the (b).

620 °C. As presented in Fig. 4, the needle valve equipped at cathode outlet was controlled to apply different pressure between the cathode and anode from 0 bar to 1.0 bar with 0.1 bar difference. While the differential pressure increased, total gas flow rate in cathode outlet was measured by digital volumetric (bubble) flowmeter (Optiflow 650, Agilent Technologies, USA), and N_2 percentage was measured by gas chromatography (7890A, Agilent Technologies, USA).

In order to demonstrate the mechanical strength of the matrix, 3-point bending test was conducted by strength measuring instrument (QC-508E, Cometech, Taiwan). Moreover, to identify improvement of mechanical strength against to cracking during the cell operation, thermal cycle test was conducted under the condition as shown in Fig. 5. Then, N_2 crossover in the anode outlet was analyzed by gas chromatography (7890A, Agilent Technologies, USA). The N_2 concentration in the anode outlet can be an indicator for how much amount of crack formed during the thermal cycling procedure.
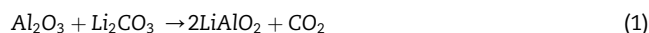
Single cell operation

Besides the out of cell tests (3-point bending test and thermal cycle test), evaluation of the stability and durability of pure α-$LiAlO_2$ matrix and Al foam-reinforced α-$LiAlO_2$ matrix during cell operation had conducted by single cell test for 1000 h. The performance was measured under 150 mA/cm^2 of current density by DC electronic loader (ESL-300Z, ELTO DC Electronics Co., Republic of Korea). Internal resistance of cell was analyzed at OCV with electrochemical impedance analyzer (SI 1287A, Solartron Analytical, USA) and frequency response analyzer (1255B, Solartron Analytical, USA). For an observation of crack formation in the matrix during the cell operation, N_2 crossover in the anode outlet was analyzed with a gas chromatography (7890A, Agilent Technologies, USA). The characteristics of single cell test components and the cell operation conditions are summarized in Table 2.

Post analysis

During the cell operation, Al_2O_3 skin layer formed on the Al foam reacted with Li_2CO_3 in the electrolyte to change into $LiAlO_2$ by the reaction (1) [4,9].

$$Al_2O_3 + Li_2CO_3 \rightarrow 2LiAlO_2 + CO_2 \tag{1}$$

Furthermore, since electrolyte management during cell operation is one of the difficult technologies for MCFC, controlling the composition of electrolyte and the total amount of electrolyte at the first cell assembling effects on the lifetime of cell immediately [12,13]. Adding aluminum in the matrix
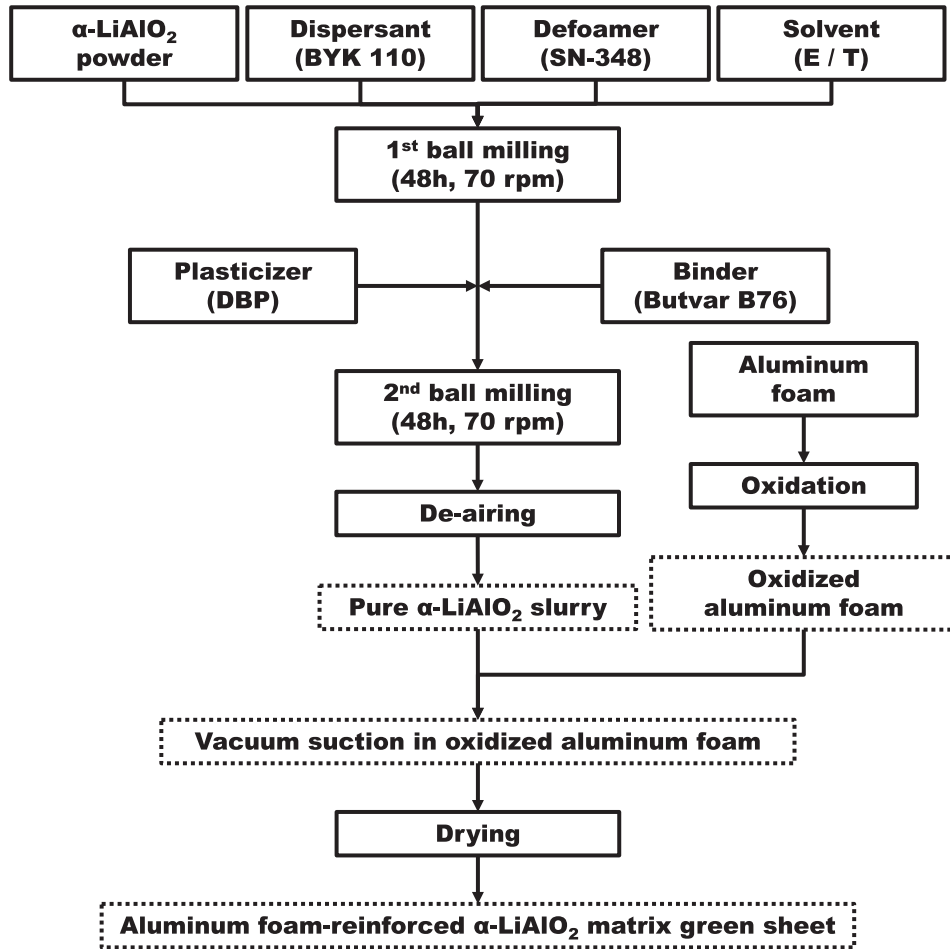
Fig. 3 — Flowchart of Al foam-reinforced α-LiAlO$_2$ matrix fabrication process.

Table 1 — Slurry composition of pure α-LiAlO$_2$ matrix to pack Al foam.

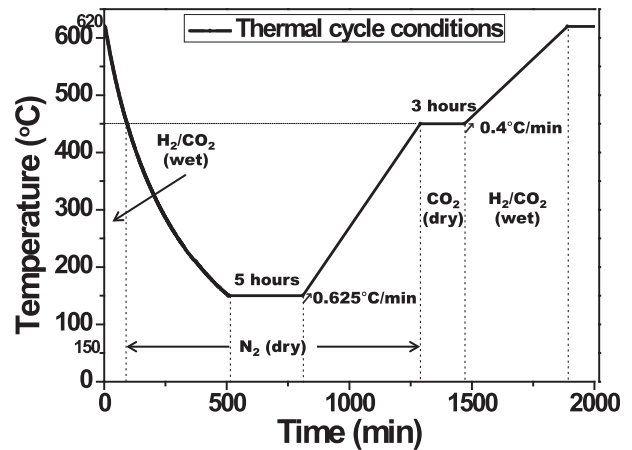| Material	Weight percent (wt. %)
α-LiAlO$_2$ powder	0.363
Binder	0.09
Plasticizer	0.058
Solvents	
Toluene	0.33
Ethanol	0.14
Dispersant	0.011
Defoamer	0.005

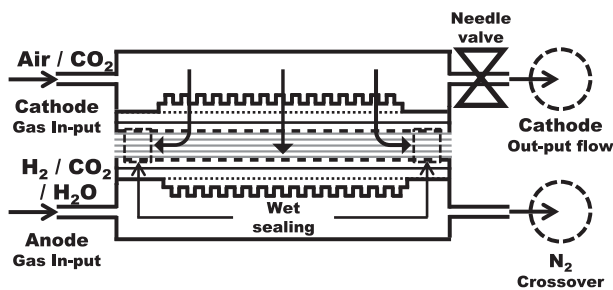Fig. 5 — Thermal cycle test conditions.

Fig. 4 — Schematic illustrations of differential pressure test set.

consumes Li$_2$CO$_3$ in the electrolyte by reaction as above in the reaction (1) after the aluminum turned to alumina from the surface causing electrolyte shortage in the single cell and accelerates degradation of cell performance.

Residual electrolyte amount and the electrolyte composition differences are examined by Atomic absorption spectroscopy, ASS (ICE 3000 series, Thermo Scientific, USA) and

Table 2 – Characteristics of single cell test components, and cell operation conditions.

MCFC single cell components		Characteristics
Anode	Size (cm × cm)	5 × 5
	Materials	Ni/Ni-5wt.%Al alloy
	Thickness (mm)	0.69–0.7
	Fuel gas (mole ratio)	H_2:CO_2:H_2O = 72:18:10
Cathode	Size (cm × cm)	4.5 × 4.5
	Materials	Lithiated NiO
	Thickness (mm)	0.69–0.7
	Oxidant gas (mole ratio)	Air:CO_2 = 70:30
Matrix	Size (cm × cm)	7.5 × 7.5
	Materials	α-$LiAlO_2$ or Al foam
	Thickness (mm)	1.2
Electrolyte	Materials	Li_2CO_3/K_2CO_3 (70/30 of mole ratio)
Cell frame	Size (cm × cm)	7.5 × 7.5
	Materials	SUS316L
Operation conditions	Temperature (°C)	620
	Pressure (atm)	1.0

Inductive coupled plasma optical emission spectrometer, ICP-OES (Varian-720ES, Algilent Technologies, USA) after operation of the cells with pure α-$LiAlO_2$ matrix and Al foam-reinforced α-$LiAlO_2$ matrix for 1000 h. Residual electrolyte amount ratio and molar ratio of electrolyte was calculated from weight percentage of Al, Li, and K [14,15]. In case of Al foam-reinforced α-$LiAlO_2$ matrix, the sample for post-analysis was obtained only from α-$LiAlO_2$ powders that were included in the Al-foam.

Results and discussion

As shown in SEM images in Fig. 6, for Al foam-reinforced α-$LiAlO_2$ matrix, $LiAlO_2$ powders were packed uniformly.

Typically, for MCFC cell operation, 50–60% of matrix porosity is considered suitable [16]. The result shown in Table 3 indicates that both matrices achieved their required porosities (56.73% for pure α-$LiAlO_2$ matrix and 51.73% for Al foam-reinforced α-$LiAlO_2$ matrix). In case of pore sizes, 0.1–0.5 μm of pore size of matrix is generally considered adequate. In order to retain the liquid electrolyte as much as possible in a matrix, the minimum pore size distribution is required for strong capillary pressure as described in Eq. (2),

$$r = \frac{2\sigma cos\theta}{\Delta P}$$ (2)

where r is the pore radius, σ is the surface tension coefficient of the electrolyte (62 mol % of Li_2CO_3 + 38 mol % of K_2CO_3), θ is the contact angle of electrolyte with the matrix and, ΔP is the pressure difference between curvatures.

From the analysis of the cumulative pore volume and median pore size demonstrated in Fig. 7 and in Table 3, we can understand that pure α-$LiAlO_2$ matrix had 0.18 μm of
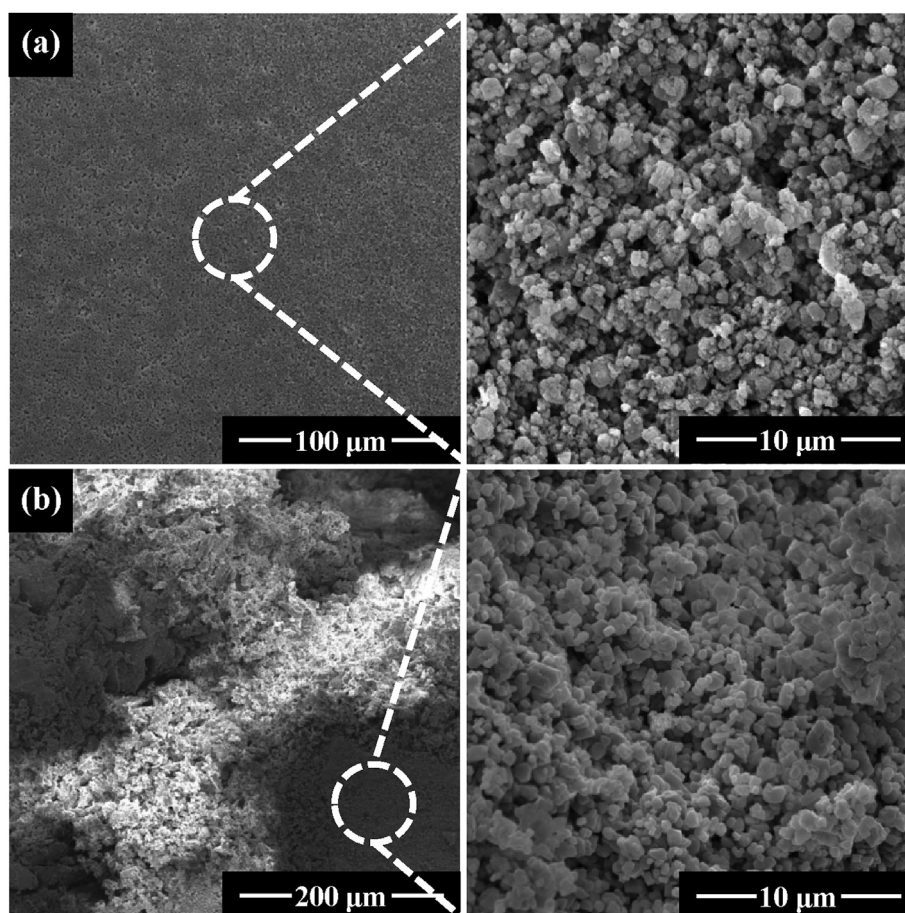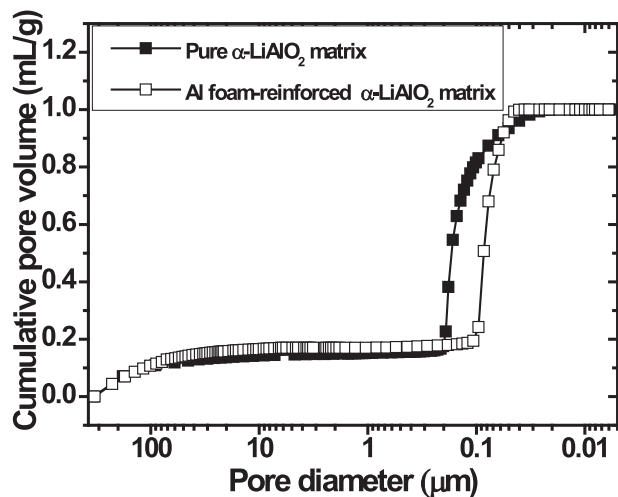

Fig. 6 – SEM images of (a) pure α-$LiAlO_2$ matrix and (b) Al foam-reinforced α-$LiAlO_2$ matrix after burn out.

Sample	Porosity (%)	Median pore size (μm)
Pure α-LiAlO₂ matrix	56.73	0.18
Al foam-reinforced α-LiAlO₂ matrix	51.73	0.09

Fig. 7 – Cumulative pore volume of pure α-LiAlO₂ matrix, and Al foam-reinforced α-LiAlO₂ matrix.

median pore size and Al foam-reinforced α-LiAlO₂ matrix had 0.09 μm. Therefore, it can be assumed that uniform and smaller pore sizes of Al foam-reinforced α-LiAlO₂ matrix suggest higher capillary force than the pure α-LiAlO₂ matrix to preserve the electrolyte in the pores of matrix. Moreover, bigger pore size of the pure α-LiAlO₂ matrix and broader pore size distribution indicate that there is a possibility of weakening of mechanical strength and loosing electrolyte during a cell operation by lack of uniformity in electrolyte distribution.

As the result presented in Fig. 8, Al foam-reinforced α-LiAlO₂ matrix shows 4.68% of N₂ crossover at 1.0 bar of differential pressure, and 3.7% of decrement in the total gas flow rate of cathode outlet while pure α-LiAlO₂ matrix shows 5.79% and 4% respectively. The lower N₂ crossover percentage and smaller total gas flow rate difference indicate that Al foam-reinforced α-LiAlO₂ matrix had preferable pore size, and size distribution to retain the electrolyte in the matrix pores in the cell operation than the pure α-LiAlO₂ matrix.

Both mechanical strength of pure α-LiAlO₂ matrix and Al foam-reinforced α-LiAlO₂ matrix were measured by 3-point bending test at the room temperature in the air. As shown in Fig. 9(a), pure α-LiAlO₂ matrix showed only 0.2 MPa of bending strength, while Al foam-reinforced α-LiAlO₂ matrix showed 1.90 MPa which means 9.4 times of strength enhancement. In addition, stress behavior of each matrix was evaluated as well by the stress in the middle of the samples when loading pin is moving down with the same speed. As demonstrated in Fig. 9(b), pure α-LiAlO₂ matrix was affected immediately by the stress and cracked in a short displacement difference.
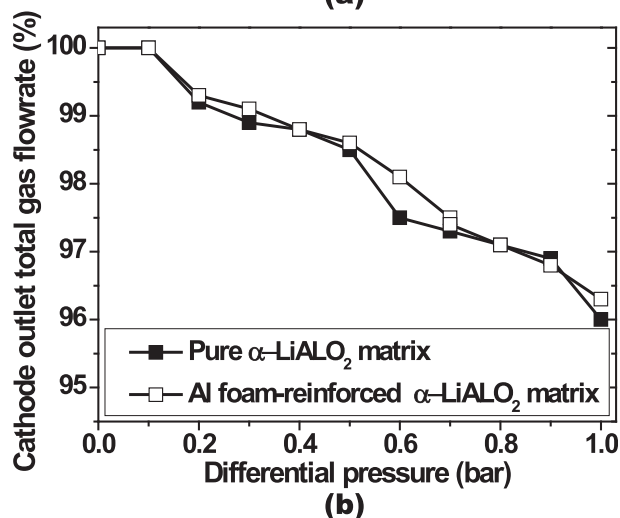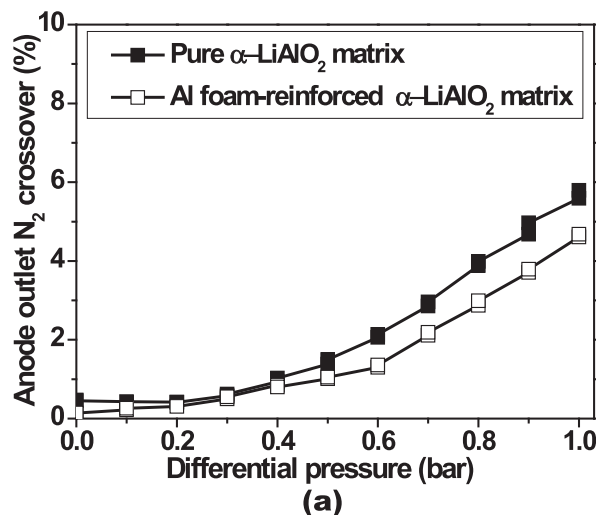
Fig. 8 – Differential pressure test: (a) anode outlet N₂ crossover (%) and (b) cathode outlet total gas flow rate (%) of pure α-LiAlO₂ matrix and Al foam-reinforced α-LiAlO₂ matrix.

However, Al foam-reinforced α-LiAlO₂ matrix was more resistive to the stress from the moving loading pin demonstrating the higher bending strength about 9.4 times.

During the thermal cycle test, the matrix is initially damaged by density difference as the electrolyte phase change occurs from liquid to solid, and then damaged again by thermal stress due to different thermal expansion coefficients of the electrodes, electrolyte, and matrix. Consequently, possibility of crack formation can increase due to the thermal stress during the thermal cycle test. Before the thermal cycle test was performed, N₂ crossovers of pure α-LiAlO₂ matrix and Al foam-reinforced α-LiAlO₂ matrix were 0.13%, and 0.10%, respectively, which is considered that matrix was not damaged and had no cracks. However, N₂ crossover of pure α-LiAlO₂ matrix increased significantly, as the thermal cycle performed. It was 0.13% before the thermal cycle, but increased to 1.95% after the second thermal cycle test. It indicates that the crack formation proceeded during the thermal cycling procedure. On the other hand, Al foam-reinforced α-LiAlO₂ matrix was durable enough to sustain the several
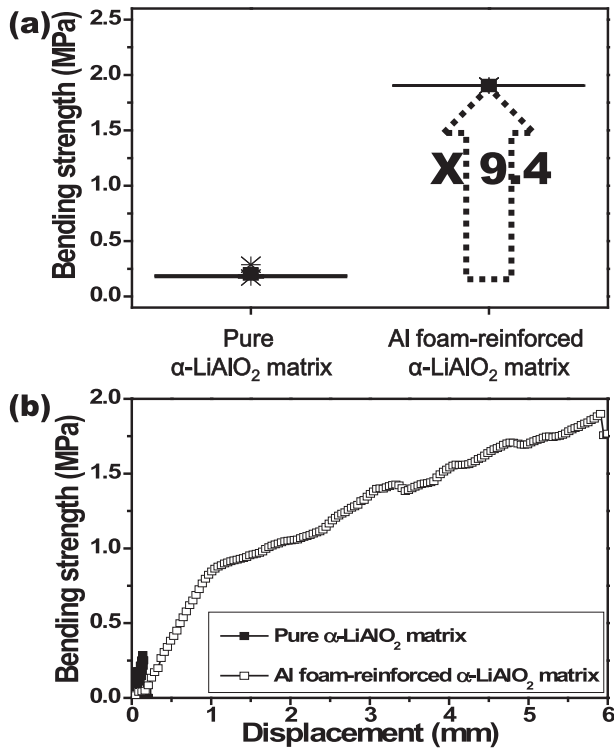
Fig. 9 — (a) Bending strength and (b) stress behavior of pure α-LiAlO₂ matrix, and Al foam-reinforced α-LiAlO₂ matrix.

Fig. 11 — Single cell performances, internal resistance, and N₂ crossover of (a) pure α-LiAlO₂ matrix and (b) Al foam-reinforced α-LiAlO₂ matrix at 620 °C.

thermal cycle tests showing 0.9% of N_2 crossover even after 13 times of thermal cycle test. It implies that the Al foam-reinforced α-LiAlO₂ matrix had higher mechanical strength and stability to prevent crack formation against to thermal stress from temperature changes. The amount of N_2 crossover in the anode outlet with different type of matrix is demonstrated in Fig. 10 as a function of numbers of thermal cycle test.

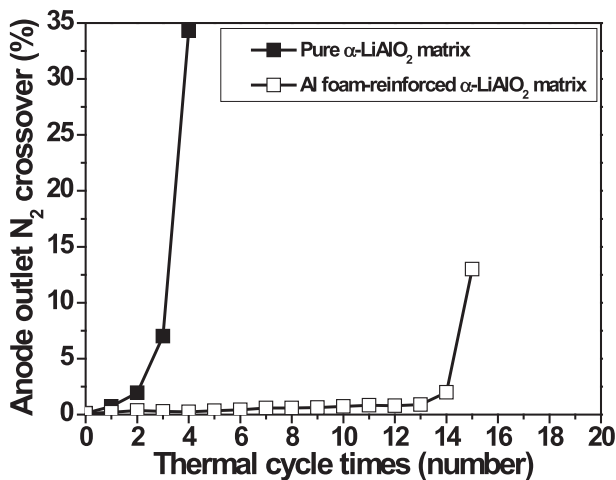The single cells with pure α-LiAlO₂ matrix and Al foam-reinforced α-LiAlO₂ matrix were operated for 1000 h, and

Fig. 10 — N₂ crossover (%) in the anode outlet of pure α-LiAlO₂ matrix, and Al foam-reinforced α-LiAlO₂ matrix by thermal cycle times.
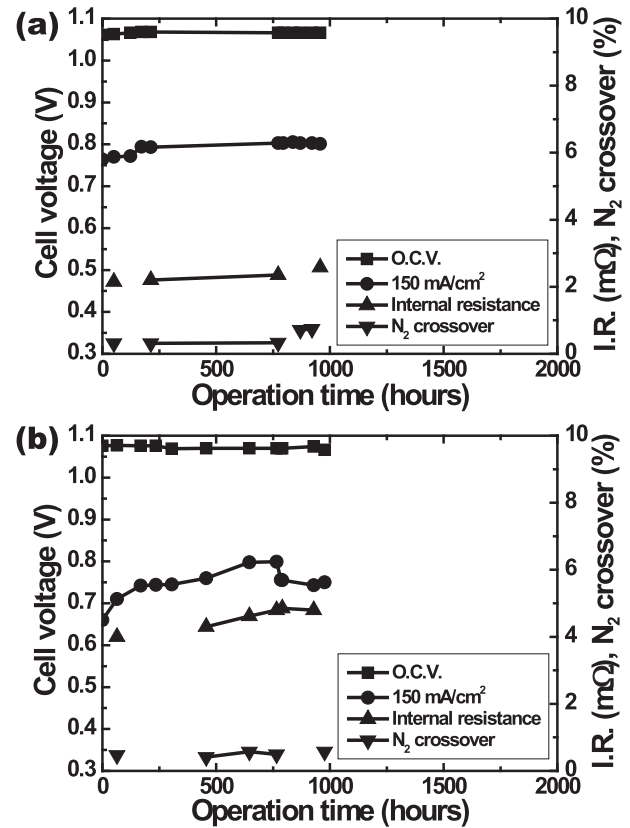
then stopped for a post-test analysis. As shown in Fig. 11, for the pure α-LiAlO₂ matrix single cell, the performance was stable. The open circuit voltage (OCV) was 1.066 V and the cell voltage was around 0.803 V at 150 mA/cm² of current density. N_2 crossover and internal resistance were steady under 0.5% and 3 mΩ, respectively until 770 h of cell operation and then started to increase after 770 h. However, the cell performance at 150 mA/cm² of current density was quite stable. It suggests that the cell performance of pure α-LiAlO₂ matrix was not affected by the increase of N_2 crossover resulting from the cracks of matrix in the short operating time of less than 1,000 h.

In case of Al foam-reinforced α-LiAlO₂ matrix, the open circuit voltage was stable in 1.072 V as well. However, the performance at 150 mA/cm² of current density was unstable. The low cell performance compared with the pure α-LiAlO₂ matrix is due to the high internal resistance. By the lithium consumption reaction as mentioned in the reaction (1) [8,9], the electrolyte can have a different electrolyte composition from the eutectic composition of 62 mol% Li_2CO_3 and 38 mol% K_2CO_3 during the cell operation. Even though the internal resistance was higher than pure α-LiAlO₂ matrix, N_2 crossover is considered acceptable in comparison with the pure α-LiAlO₂ matrix for long-term cell operation.

From XRD results described in Fig. 12, besides alpha and gamma phases of LiAlO₂ were observed after the cell operation in both pure α-LiAlO₂ matrix and Al foam-reinforced α-
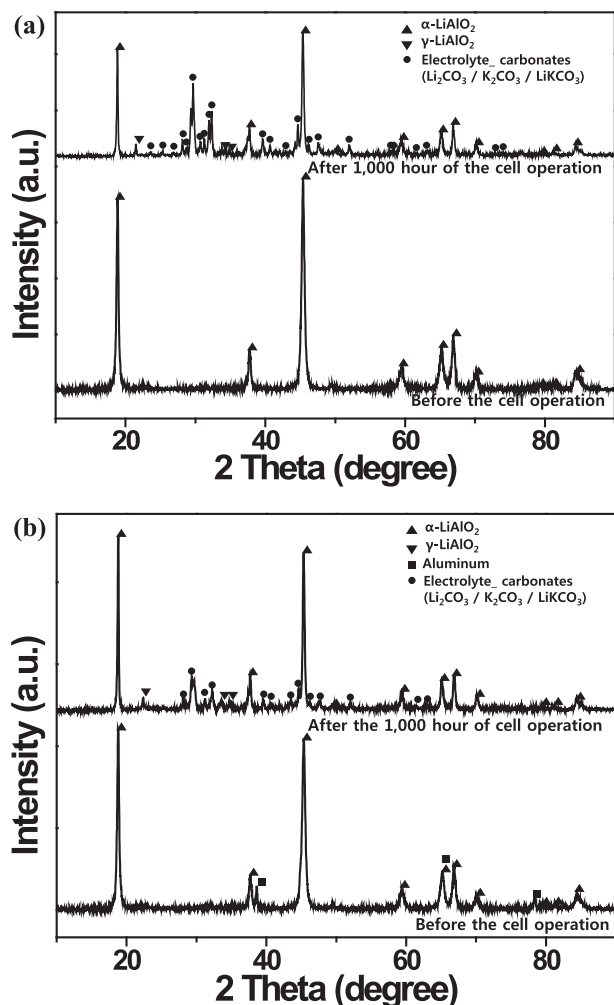
Fig. 12 − XRD patterns of (a) pure α-LiAlO₂ matrix, and (b) Al foam-reinforced α-LiAlO₂ matrix; before the cell operation and after the 1,000 h of cell operation.

Table 4 − Relative total amount and molar ratio of electrolyte after cell operation.

Sample	Weight percent			Molar ratio (mol)	
	Al	Li	K	Li_2CO_3	K_2CO_3
Pure α-LiAlO₂ matrix	18.4	9.85	11.2	0.72	0.28
Al foam-reinforced α-LiAlO₂ matrix	26.2	8.99	8.29	0.60	0.40

reduced amount of electrolyte and the change of electrolyte composition due to lithium consumption by the reaction (1) induced higher internal resistance and lower cell performance. However, if the lithium consumption was minimized by addition of excess Li_2CO_3 in the Al-foam matrix, it is expected that the Al foam support can reinforce the mechanical strength of matrix and enhance the stack lifetime for MCFCs [15,19].

Conclusions

In this study, Al foam-reinforced matrix was developed to enhance the mechanical strength. In microstructure characterization, Al foam-reinforced α-LiAlO₂ matrix had porosity of 51.7% and median pore size of 0.085 μm which are adequate for a matrix of MCFCs. Moreover, electrolyte retention capability in the pores was estimated to be suitable by differential pressure test. The Al foam-reinforced α-LiAlO₂ matrix had appropriate pore size for cell operation, resulting in lower N_2 crossover percentage in anode outlet and smaller gas flow rate difference in cathode outlet than the pure α-LiAlO₂ matrix. In addition, mechanical strength of Al foam-reinforced α-LiAlO₂ matrix had improved about 9.4 times in bending strength and showed higher resistance against to thermal stress caused by temperature difference in thermal cycle test compared to pure α-LiAlO₂ matrix. In the single cell test, pure α-LiAlO₂ matrix showed stable performance in short operating time. However, due to the poor mechanical strength of matrix, the N_2 crossover increased after 770 h operation. In case of Al foam-reinforced α-LiAlO₂ matrix, the mechanical strength was greatly enhanced 9.4 times. The cell performance was not good compared to the standard cell with pure α-LiAlO₂ matrix due to the high internal resistance caused by electrolyte consumption, especially the lithium carbonate loss. In this work, the Al foam support can reinforce the mechanical strength of matrix and enhance the stack lifetime for MCFCs. However, the reduced amount of electrolyte and the change of electrolyte composition due to lithium consumption induced higher internal resistance and lower cell performance. Further study on lithium consumption is required to prevent the lithium carbonate loss.

LiAlO₂ matrix, it is supposed that alpha and gamma phase change had no effect on cell performance because of small concentration of gamma LiAlO₂ and relatively short operation time [17,18].

After the cell operation, the matrix samples were collected and analyzed by ICP and AAS. From the results, the Li_2CO_3 loss and the molar ratio of Li_2CO_3 and K_2CO_3 were calculated. According to the XRD results in Fig. 12, it can be presumed that there was no new compound and LiAlO₂, Li_2CO_3, and K_2CO_3 were the main chemicals after the cell operation for 1,000 h. In Table 4, molar ratio of Li_2CO_3, and K_2CO_3 were calculated from the result of the weight percent by ICP and AAS analysis.

From the ICP and AAS results, it is clear that the electrolyte composition changed in the Al foam-reinforced α-LiAlO₂ matrix. Moreover, 8 wt.% of Li_2CO_3 in the amount of original electrolyte (62 mol%Li_2CO_3/38 mol%K_2CO_3) was consumed by the formation of lithium aluminate with Li_2CO_3 and Al_2O_3 in Al-foam through the reaction (1). It is assumed that the Li_2CO_3 depletion in the matrix caused the low cell performance compared to the pure α-LiAlO₂ matrix. Consequently, the

REFERENCES

[1] Hengeveld DW, Revankar ST. Economic analysis of a combined heat and power molten carbonate fuel cell system. J Power Sources 2007;165:300—6.

[2] Selman JR. Molten-salt fuel cells—technical and economic challenges. J Power Sources 2006;160:852—7.

[3] Freni S, Cavallaro S, Aquino M, Ravida D, Giordano N. Lifetime-limiting factors for a molten carbonate fuel cell. Int J Hydrogen Energy 1994;19:337—41.

[4] Lee J-J, Choi H-J, Hyun S-H, Im H-C. Characteristics of aluminum-reinforced γ-LiAlO$_2$ matrices for molten carbonate fuel cells. J Power Sources 2008;179:504—10.

[5] Ham HC, Yoon SP, Han J, Nam SW, Lim T-H, Hong S-A. Development of reinforced matrix for molten carbonate fuel cells by using sintering aids. ECS Trans 2007;5:445—9.

[6] Lee I, Kim W, Moon Y, Lim H, Lee D. Influence of aluminum salt addition on in situ sintering of electrolyte matrices for molten carbonate fuel cells. J Power Sources 2001;101:90—5.

[7] Kim H-S, Song S, Jang S-C, Park D-N, Ham H-C, Yoon S-P, et al. Enhancement of mechanical strength using nano aluminum reinforced matrix for molten carbonate fuel cell. Trans Korean Hydrogen New Energy Soc 2012;23:143—9.

[8] Kim J-E, Han J, Yoon SP, Nam SW, Lim T-H, Kim H. Mechanical properties of the lithium aluminate matrix for MCFC reinforced with metal oxide materials. Curr Appl Phys 2010;10:S73—6.

[9] Kim J-E, Patil KY, Han J, Yoon S-P, Nam S-W, Lim T-H, et al. Using aluminum and Li$_2$CO$_3$ particles to reinforce the α-LiAlO$_2$ matrix for molten carbonate fuel cells. Int J Hydrogen Energy 2009;34:9227—32.

[10] Patil KY, Yoon SP, Han J, Lim T-H, Nam SW, Oh I-H. The effect of lithium addition on aluminum-reinforced α-LiAlO$_2$ matrices for molten carbonate fuel cells. Int J Hydrogen Energy 2011;36:6237—47.

[11] Choi H-J, Lee J-J, Hyun S-H, Lim H-C. Fabrication and performance evaluation of electrolyte-combined α-LiAlO$_2$ matrices for molten carbonate fuel cells. Int J Hydrogen Energy 2011;36:11048—55.

[12] Nam S-W, Lim T-H, Oh I-H, Lee K-S, Yoon S-P, Hong S-A, et al. Performance of a small-scale molten carbonate fuel cell stack I: performance of a 100W-class cross-flow type stack. Korean Chem Eng Res 1995;33:559.

[13] Tanimoto K, Yanagida M, Kojima T, Tamiya Y, Matsumoto H, Miyazaki Y. Long-term operation of small-sized single molten carbonate fuel cells. J Power Sources 1998;72:77—82.

[14] Kulkarni A, Giddey S. Materials issues and recent developments in molten carbonate fuel cells. J Solid State Electrochem 2012;16:3123—46.

[15] Morita H, Kawase M, Mugikura Y, Asano K. Degradation mechanism of molten carbonate fuel cell based on long-term performance: long-term operation by using bench-scale cell and post-test analysis of the cell. J Power Sources 2010;195:6988—96.

[16] Zhou L, Lin H, Yi B. Sintering behavior of porous α-lithium aluminate matrices in molten carbonate fuel cells at high temperature. J Power Sources 2007;164:24—32.

[17] Tomimatsu N, Ohzu H, Akasaka Y, Nakagawa K. Phase stability of LiAlO$_2$ in molten carbonate. J Electrochem Soc 1997;144:4182—6.

[18] Terada S, Nagashima I, Higaki K, Ito Y. Stability of LiAlO$_2$ as electrolyte matrix for molten carbonate fuel cells. J Power Sources 1998;75:223—9.

[19] Youn JY, Yoon SP, Han J, Nam SW, Lim T-H, Hong S-A, et al. Fabrication and characteristics of anode as an electrolyte reservoir for molten carbonate fuel cell. J Power Sources 2006;157:121—7.